Homologous Mutations on Different Subunits Cause Unequal but Additive Effects on *n*-Alcohol Block in the Nicotinic Receptor Pore

Stuart A. Forman
Department of Anesthesia, CLN-3, Massachusetts General Hospital, Boston, Massachusetts 02114 USA

ABSTRACT Hydrophobic antagonists of the nicotinic acetylcholine receptor inhibit channel activity by binding within the transmembrane pore formed by the second of four transmembrane domains (M2) on each of the receptor's subunits. Hydrophobic mutagenesis near the middle (10′ locus) of the α-subunit M2 domain results in channels that are much more sensitive to block by long-chain alcohols and general anesthetics, indicating that the inhibitory site on wild-type receptors is nearby. To determine whether other receptor subunits also contribute to the blocker site, the hydrophobic mutagenesis strategy was extended to all four subunits at 10′ loci. αS10′I causes the largest increase in apparent hexanol binding (4.3-fold compared to wild type), approximately twice the size of the change caused by βT10′I (2.2-fold). γA10′I and δA10′I mutations cause much smaller changes in apparent hexanol binding affinity (about 1.2-fold each), even when corrected for their smaller degree of side-chain hydrophobicity changes. When 10′I mutant subunits are coexpressed, the change from wild type in apparent hexanol binding energy ($\Delta\Delta G_{mixture}$) is roughly equal to the sum of hexanol binding energy changes for the constituent mutant subunits ($\Sigma\Delta\Delta G_{subunits}$). The simplest model consistent with these results is one in which hydrophobic blockers make simultaneous contact with all five M2 10′ residues, but the extent of contact is much greater for the α and β than for γ and δ side chains.

INTRODUCTION

Hydrophobic inhibitors of the nicotinic acetylcholine receptor (nAChR) act, in part, by binding to a discrete site within the receptor's pore. Evidence for this site comes from single-channel and macroscopic kinetic data, pharmacological studies of drug interactions, and site-directed mutagenesis. Single nAChR channel patch-clamp currents in the presence of long-chain alcohols and general anesthetics show brief closures, suggesting blockade of the open channel (Lechleiter and Gruener, 1984; Dilger et al., 1991), although this state is not exclusively affected (Dilger and Brett, 1991). Macroscopic voltage-clamp currents from muscle end plates or excised membrane patches in the presence of hydrophobic blockers demonstrate two inactivation phases; the fast phase is thought to represent diffusion-limited blockade of the open channel state, and the slower phase represents receptor desensitization (Adams, 1976; McLarnon et al., 1988; Forman et al., 1995). Apparent competition between two long-chain alcohols for a saturable channel-inhibiting site is observed in rapid flux studies of nAChR-rich vesicles from *Torpedo* electroplaque (Wood et al., 1995). Site-directed mutagenesis of amino acid side chains near the center of putative pore-forming nAChR protein domains changes the pore's sensitivity to block by general anesthetics and long-chain alcohols (Forman et al., 1995).

Structural models of the nAChR pore provide a framework for probing the extent of the hydrophobic inhibitor binding site. Enhanced electron micrographic analysis of nAChR from *Torpedo* demonstrates an overall molecular structure with a central channel surrounded by pentagonally arranged protein (Unwin, 1993; Kistler et al., 1982). Photolabeling of *Torpedo* nAChR protein and site-directed mutagenesis of *Torpedo* nAChR and homologous vertebrate nAChRs identify a set of amino acids in the second of four predicted transmembrane domains (M2) in each receptor subunit (stoichiometry $\alpha_2\beta\gamma\delta$) that interact with translocated ions as well as blockers (Giraudat et al., 1986, 1987; Hucho et al., 1986; Pedersen et al., 1992; Imoto et al., 1988, 1991; Leonard et al., 1988; Imoto et al., 1991; Cohen et al., 1992b; Villarroel et al., 1991). The high degree of amino acid sequence homology among the nAChR subunit M2 domains (see Table 1) and site-directed mutagenesis studies showing that homologous mutations have similar effects on different subunits leads most researchers to incorporate a fivefold symmetry assumption into their models of the nAChR channel (Karlin et al., 1986; Charnet et al., 1990; Finer-Moore and Stroud, 1984; Filatov and White, 1995; Devillers-Thiery et al., 1993; Sankararamakrishnan et al., 1996). In these models, homologous positions (aligned from 1′ to 20′, as shown in Table 1) on each subunit M2 domain form functional "rings" along the transmembrane axis (Imoto et al., 1988; Miller, 1989; Charnet et al., 1990; Devillers-Thiery et al., 1993).

In previous site-directed mutagenesis experiments (Forman et al., 1995), changing the hydrophobicity of amino acid side chains near the middle of the M2 domain in the mouse muscle nAChR α-subunit was used as a test for interactions of these residues with isoflurane, hexanol, and octanol. As the serine (S) residue at α10′ is mutated to the more hydrophobic amino acids valine (αS10′V), isoleucine (αS10′I), and phenylalanine (αS10′F), a graded increase in

Received for publication 25 November 1996 and in final form 28 January 1997.

Address reprint requests to Dr. Stuart A. Forman, CLN-3, Massachusetts General Hospital, Boston, MA 02114. Tel.: 617-726-1677; Fax: 617-726-5748; E-mail: forman@helix.mgh.harvard.edu.

0006-3495/97/05/2170/10 $2.00

TABLE 1 Amino acid sequences of mouse muscle M2 domains*

		1′	2′	3′	4′	5′	6′	7′	8′	9′	10′	11′	12′	13′	14′	15′	16′	17′	18′	19′	20′
α	K242	M	T	L	S	I	S	V	L	L	S	L	T	V	F	L	L	V	I	V	E
β	K253	M	G	L	S	I	F	A	L	L	T	L	T	V	F	L	L	L	L	A	D
γ	K251	C	T	V	A	T	N	V	L	L	A	Q	T	V	F	L	F	L	V	A	K
δ	K256	T	S	V	A	I	S	V	L	L	A	Q	S	V	F	L	L	L	I	S	K

*Sequence alignment and terminology follow that of Miller (1989). The first residue is numbered from the amino terminus, which is supposed to be at the cytoplasmic end of the pore. Single-letter amino acid code: A, alanine; C, cysteine; D, aspartate; E, glutamate; F, phenylalanine; G, glycine; H, histidine; I, isoleucine; K, lysine; L, leucine; M, methionine; N, asparagine; P, proline; Q, glutamine; R, arginine; S, serine; T, threonine; V, valine; W, tryptophan; Y, tyrosine.

the nAChR sensitivity to block by these molecules is observed (K_{hex}(wt)/K_{hex}(mut) ≈ 2, 4.5, and 8, respectively). In contrast to the results at 10′ loci, mutating serine to phenylalanine at a site closer to the cytoplasmic end of M2 (αS6′F) causes only a 40% change in receptor sensitivity to alcohols, suggesting that hydrophobic inhibitors interact weakly at this level in the channel. When a second mutation at the 10′ level, βS10′I, is coexpressed with αS10′I, the resulting double mutant demonstrates a 10-fold increased sensitivity to hexanol (compared to wild type), indicating that both α- and β-subunits may contribute to binding.

To further characterize the extent of the hydrophobic inhibitor site at the M2 10′ "ring" in the nAChR pore, the present study extends the hydrophobic mutagenesis approach to include all subunits of mouse muscle nAChR. Two major questions are addressed: 1) Do each of the subunit 10′ residues interact equally with hydrophobic inhibitors in the pore, as predicted by fivefold symmetry in the channel? and 2) Do the nAChR subunits form independent sites that compete for drug binding, or is there a single site that interacts simultaneously with all of the subunits?

Wild-type residues at the 10′ loci of M2 domains on each of the four subunits were mutated to isoleucines. Receptor sensitivities to acetylcholine and long-chain alcohols (hexanol or octanol) were assessed with voltage-clamped membrane patches from *Xenopus* oocytes that expressed the four subunits (mutant and wild type in all possible combinations) of mouse muscle nAChR. Submillisecond concentration jumps of agonist and/or alcohols were used to elicit currents from patches expressing receptors.

The results show that M2 10′ residues on different subunits contribute different amounts of binding energy to long-chain alcohols at the inhibition site. Both α- and β-subunit M2 10′ side chains make approximately equal contact with hydrophobic blockers bound in the nAChR pore. The γ- and δ-subunit 10′ side chains interact much more weakly with hydrophobic blockers, indicating asymmetry in the nAChR channel structure at the 10′ level. When mutations on more than one subunit are coexpressed, the individual subunit contributions to hexanol binding energy are found to be approximately additive. This result is most simply explained by a single central blocker site within the pore.

MATERIALS AND METHODS

Site-directed mutagenesis

cDNAs for α-, β-, γ-, and δ-subunits of the mouse muscle nAChR (from Dr. James Boulter) were subcloned into pSP64 plasmids containing *Xenopus* globin noncoding sequences (pSP64T; Krieg and Melton, 1984) and generously supplied by Dr. James McLaughlin (Tufts Medical School). The αS10′I mutant cDNA was made by oligonucleotide-directed mutagenesis, as described previously (Forman et al., 1995). The βT10′I mutant cDNA was provided by Cesar Labarca (California Institute of Technology) in pGEM2-SP6. Oligonucleotide-directed mutations in γ- and δ-subunit cDNAs were made using high-fidelity polymerase chain reaction (Vent enzyme; New England Biolabs) by the technique of Nelson and Long (1989). Polymerase chain reaction fragments containing mutated M2 domain sequences were exchanged for wild-type subunit sequences between *Bst*XI and *Nco*I sites in the γ-subunit and *Kpn*I and *Bsg*I sites in the δ-subunit. All mutations and transferred sequences were confirmed by dideoxynucleotide sequencing.

Xenopus oocyte expression

Methods for oocyte expression were described previously (Tomaselli et al., 1991). Messenger RNAs were in vitro transcribed using SP6 RNA polymerase kits (Ambion, Austin, TX) from linearized cDNAs. Subunit mRNAs were isolated using affinity beads (RNAid; BIO-101, Vista, CA), mixed stoichiometrically at 2α:β:γ:δ, and microinjected into oocytes (25–50 nl). After incubation for 48–72 h, oocytes were stripped of their vitelline membranes and used for electrophysiology.

Patch-clamp electrophysiology

Experiments were performed at room temperature (20–22°C). Patch pipettes were fire-polished to give an open tip resistance of 2–5 MΩ. Oocyte membrane patches were pulled in the outside-out configuration and held at −50 mV. Inside and outside buffers were symmetrical K-100 (in mM: 97 KCl, 1 $MgCl_2$, 0.2 EGTA, 5 K-HEPES, pH 7.5). Currents through the patch-clamp amplifier (Axopatch 200A; Axon Instruments, Foster City, CA) were filtered (8-pole bessel, 2–5 kHz) and digitized at 5–10 kHz using a 586-class PC, a 12-bit A/D converter (National Instruments, Austin, TX), and custom software.

Rapid perfusion

Rapid perfusate switching (0.2–1.2 ms, measured with open pipette junction currents) was achieved using either the method of Liu and Dilger (1991) or a piezo-driven theta tube. Patches were continuously perfused with K-100 buffer (with or without alcohol), until a computer-controlled signal switched the perfusate to K-100 containing ACh with or without alcohol. For alcohol concentration-response experiments, saturating concentrations of ACh (> 10 × measured K_{ACh}) were used to activate channel

openings. ACh exposure periods were between 50 and 350 ms, and patches were "recovered" in control perfusate for 5–10 s between ACh exposures.

Data analysis

Current traces displayed in figures are averages of 8–16 traces from a single patch aligned at the midpoints of the rapid current rise (channel opening). Control currents (ACh alone) were checked before and after experiments where patches were exposed to anesthetics. Data were not analyzed if the pre- and postcontrol peak currents differed by more than 10%. Nonlinear least-squares fits and Student's *t*-test analyses were performed using Origin software (Microcal, Northampton, MA).

Inhibitors

Octanol and hexanol (puriss. grade, Fluka Chemical) were weighed directly into K-100 buffer to make stock solutions that were diluted to the final experimental concentrations.

RESULTS

Subunit 10′I mutation effects on channel gating

When each 10′I mutant subunit is expressed together with the other three wild-type subunits, their effects on both ACh gating and channel inhibition by alcohols are distinctly different. Gating parameters (apparent K_{ACh}, desensitization rate (τ_{des}), mean single-channel open lifetimes, and single-channel conductance) for wild-type nAChR and each single-subunit mutant nAChR are summarized in Table 2. As reported previously (Forman et al., 1995), αS10′I causes a small (less than twofold) increase in apparent ACh affinity, increases the desensitization rate (τ_{des}), and reduces potassium conductance by less than 10%. αS10′I has no significant effect on mean open channel lifetime. In contrast, the βT10′I mutant decreases apparent ACh affinity, has little effect on desensitization, reduces the mean open channel lifetime by nearly 50%, and reduces conductance by about 12%. γA10′I and δA10′I both cause large (six- to ninefold) increases in apparent ACh affinity. γA10′I shows faster desensitization than wild type, whereas δA10′I has slower desensitization. The γA10′I mutation increases the mean open channel lifetime to 4.6-fold that of wild-type receptors. Thus, as characterized by ACh gating, each homologous subunit mutation causes a distinct pattern of changes.

Subunit 10′I mutation effects on channel inhibition by alcohols

Homologous mutations (S→A, T→A, and A→S) at 10′ loci on all four mouse muscle nAChR subunits were reported to cause small but roughly equal effects on the affinity of a charged amphipathic channel blocker, QX-222 (Charnet et al., 1990), suggesting that the 10′ residues form a symmetrical ring surrounding the blocker molecule. In contrast, the mutation of each 10′ residue to the bulky hydrophobic isoleucine side chain results in clearly unequal effects on *n*-alcohol inhibition. At concentrations of either octanol (Fig. 1, *top*) or hexanol (Fig. 1, *middle* and *bottom*) that block roughly half of the wild-type currents, the different subunit 10′I mutants are blocked to different degrees. The αS10′I mutant is the most sensitive, demonstrating a 4.3-fold increase in sensitivity to hexanol over wild type (average of 3–5 hexanol concentration responses for each 10′I mutant). βT10′I causes about half the sensitivity increase seen with αS10′I (2.2-fold), whereas γA10′I and δA10′I each increase hexanol sensitivity by ~1.2-fold. Average K_{hex} ratios were used to calculate changes in free energy for hexanol block for each mutant, displayed in Fig. 2. The averaged $\Delta\Delta G$ values for γA10′I and δA10′I are significantly different from zero ($p < 0.05$).

A possible explanation for why the γA10′I and δA10′I mutations cause smaller changes in apparent hexanol sensitivity than αS10′I and βT10′I mutations is that the relative change in hydrophobicity between alanine and isoleucine side chains is less than that between serine and isoleucine. To correct for this inequality, both γA10′S and δA10′S mutant receptors were expressed and their hexanol sensitivities measured. As predicted from the reduced hydrophobicity of the 10′ side chain, both of these mutant receptors show slightly lower sensitivity to hexanol than the wild-type

TABLE 2 Gating properties[#] of receptors with single subunit 10′I mutations

Receptor	K_{ACh} (μM)	γ (pS)	Mean open time (ms)	τ_{des} (ms)
WT	18 ± 2	48 ± 1	3.7 ± 0.5	120 ± 30
αS10′I	10 ± 2	44 ± 1	4.1 ± 0.5	30 ± 10
βT10′I	50 ± 5	42 ± 1	1.9 ± 0.3	100 ± 30
γA10′I	2.0 ± 0.3	42 ± 1	17 ± 2	70 ± 20
δA10′I	3.0 ± 0.5	ND	ND	200 ± 50

[#] K_{ACh} values for each channel type were determined by measuring average (eight events) peak current responses in outside-out patches ($V_m = -50$ mV) during rapid perfusion with varying ACh concentrations (range 0.1 μM to 1 mM). Responses were normalized to average control currents measured with saturating ACh concentrations (0.1–1 mM) in the same patch. A logistic function, $I/I_{cont} = [ACh]^{nH}/([ACh]^{nH} + K_{ACh}{}^{nH})$, was fitted to data points from at least three patches at each concentration. Single-channel conductances for each channel type (γ) were measured in excised inside-out patches held at −50 or −100 mV. The concentration of ACh in the patch pipette was 200 nM to 1 μM. Fifty single-channel conductances from at least three patches were averaged. Single-channel mean open times were determined by fitting a single exponential decay function to frequency histograms of the durations of 100–150 sequential openings. Desensitization time constants (τ_{des}) for each channel type were determined by recording averaged (eight events) currents from outside-out membrane patches during rapid perfusion with 500 μM ACh. Perfusion periods were lengthened for slowly desensitizing receptors (e.g., wild type). Single exponential functions were fitted to the current decay phases. Between 5 and 15 fitted decay constants were averaged.

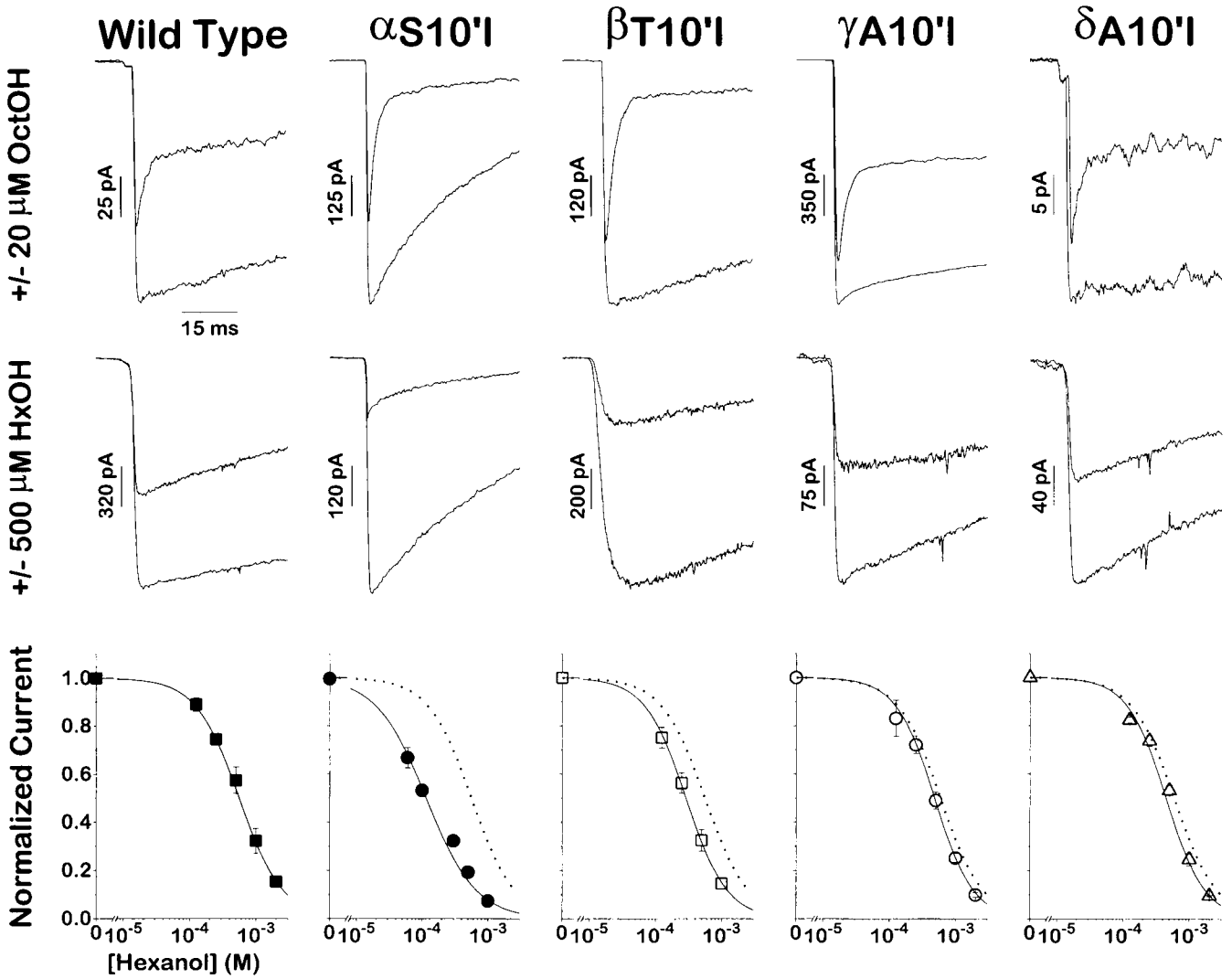

FIGURE 1 Effects of homologous hydrophobic mutations on receptor-alcohol interactions. Each panel represents data from a different oocyte patch expressing wild-type or mutant receptor subunits as labeled. (*Top*) Averaged (8–16 events) patch current traces in the absence and presence of 20 μM octanol. Currents were elicited with 0.2–1.0 mM ACh (at least 10 × K_{ACh}), and octanol was present in both control and ACh perfusates. Rapid octanol inhibition after ACh exposure is observed in all receptors. Values for steady-state block by octanol determined from double exponential fits were as follows: wt, 58%; αS10'I, 85%; βT10'I, 83%; γA10'I, 55%; δA10'I, 56%. (*Middle*) Averaged patch current traces in the absence and presence of 500 μM hexanol. Currents were elicited with ACh at least 10 × K_{ACh}, and hexanol was present in both control and ACh perfusates. Values for peak current block by hexanol were as follows: wt, 41%; αS10'I, 78%; βT10'I, 72%; γA10'I, 52%; δA10'I, 48%. (*Bottom*) Hexanol concentration responses obtained from single patches. Perfusion conditions were as described above, and normalized currents were calculated by dividing peak currents in the presence of hexanol to control peak currents without hexanol. Error bars represent the standard deviation of averaged data at a single hexanol concentration (at least three exposures). Logistic functions ($F = 1 - [\text{Hex}]^{nH}/\{[\text{Hex}]^{nH} + K_{hex}{}^{nH}\}$) were fit to data (shown as *solid lines*). Mutant traces are paired with wild-type experiments performed on the same day (represented by *dotted lines*). Fitted parameters: wild type, K_{hex} = 560 ± 30 μM, n_H = 1.3 ± 0.1; αS10'I, K_{hex} = 120 ± 20 μM, n_H = 1.1 ± 0.1; βT10'I, K_{hex} = 290 ± 20 μM, n_H = 1.4 ± 0.1; γA10'I, K_{hex} = 480 ± 30 μM, n_H = 1.5 ± 0.1; δA10'I, K_{hex} = 450 ± 20 μM, n_H = 1.5 ± 0.1.

nAChR (K_{hex}(mut)/K_{hex}(wt) ≈ 0.85). Thus their average $\Delta\Delta G$ values (Fig. 2, *hatched bars*) are positive, although they are not significantly different from wild type at p = 0.05 (p = 0.09 and 0.052 for γA10'S and δA10'S, respectively). By subtracting $\Delta\Delta G$ values for the γ and δ 10'S mutants from those for the respective 10'I mutants, the $\Delta\Delta G$ value for the serine-to-isoleucine substitution was estimated (Fig. 2, *cross-hatched bars*). Even with these corrections for unequal mutations, the $\Delta\Delta G$ values derived for the γ- and δ-subunits are significantly lower than that for the βT10'I mutation.

Despite their different contributions to hexanol binding energy, each of the 10'I mutant nAChRs maintains the apparent open-channel selective block mechanism seen in the wild-type nAChR. This is evident from the rapid octanol inhibition phases (Fig. 1, *top*) in current traces from patches that were preequilibrated with octanol. This fast phase is not seen with hexanol because it is present at a 25-fold higher

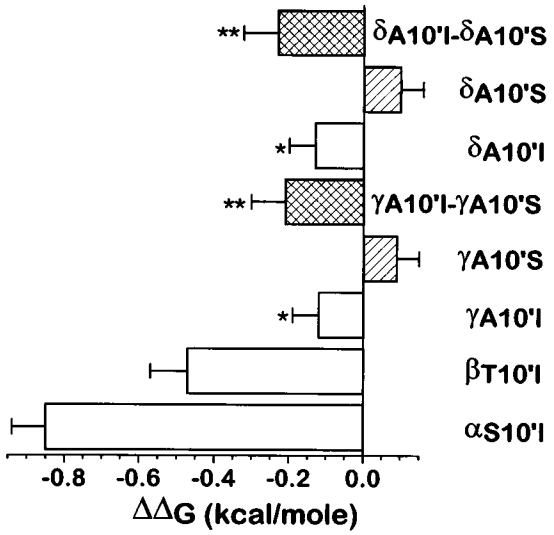

FIGURE 2 Apparent mutation-induced changes in hexanol binding energy. $\Delta\Delta G$ values were calculated as $\Delta\Delta G = -RT \times \ln[K_{hex}(mut)/K_{hex}(wt)]$ from individual experiments (e.g., Fig. 1, *bottom*). Three to five such values for each mutant were averaged and are plotted with error bars representing the standard error of the mean. □, $\Delta\Delta G$ values for 10′I mutants; ▨, 10′S mutants. Bars labeled γA10′I-γA10′S and δA10′I-δA10′S (▩) represent the difference between respective 10′I and 10′S bars. *Significantly different from wild type ($\Delta\Delta G = 0.0 \pm 0.05$) at $p \leq 0.05$. **Significantly different from β10′I value at $p \leq 0.01$.

concentration than octanol, which has a k_{on} of $10^7\ M^{-1}\ s^{-1}$ (Forman et al., 1995). Channel block by 500 μM hexanol is predicted to reach equilibrium in about 200 μs, near the rise time in the fastest patch currents.

The rate of inhibition at αS10′I receptors was measured over a range (4–40 μM) of octanol concentrations. The apparent on and off rates for octanol were determined to be $(9 \pm 2) \times 10^6\ M^{-1}\ s^{-1}$ and $80 \pm 20\ s^{-1}$, respectively (data not shown). Thus, compared to kinetics in wild-type nAChR, this mutation reduces the apparent k_{off} for octanol, but has little effect on k_{on}.

Additive effects of subunit 10′I mutations on alcohol inhibition

Hydrophobic inhibitors in the nAChR channel may occupy a central position at which simultaneous contact with all of the subunits occurs. Alternatively, the nAChR channel lining may form multiple independent sites where anesthetics can bind and inhibit ion movement. To determine which of these models is correct, the additive effects of subunit 10′I mutations on hexanol binding were assessed. If coexpression of mutant subunits demonstrates energy additivity with regard to *n*-alcohol inhibition, then simultaneous contact with all subunits must be occurring. The existence of independent sites that compete for hydrophobic blocker binding predicts that coexpression of mutant subunits will result in less-than-additive energy contributions from each subunit (Heginbotham and MacKinnon, 1992).

All possible combinations of two (six combinations), three (four combinations), and four (one combination) 10′I mutant subunit cRNA types were mixed with wild-type subunit cRNAs (to provide all four subunit types) and expressed in *Xenopus* oocytes. Each combination mutant was characterized by measuring hexanol concentration responses (in three to five separate patches) in parallel with a wild-type nAChR concentration response for hexanol done on the same day. K_{hex} was calculated by fitting a logistic function to data points representing inhibition of peak currents by hexanol. The resulting K_{hex} values for mutant combinations and wild-type controls were used to calculate $\Delta\Delta G_{mixture}$, as described for single-subunit mutant receptors in Fig. 2.

In Fig. 3, calculated $\Delta\Delta G_{mixture}$ values are represented by cross-hatched bars. Paired with each of these bars is a stack of bars representing the sum of each mutant subunit's $\Delta\Delta G$

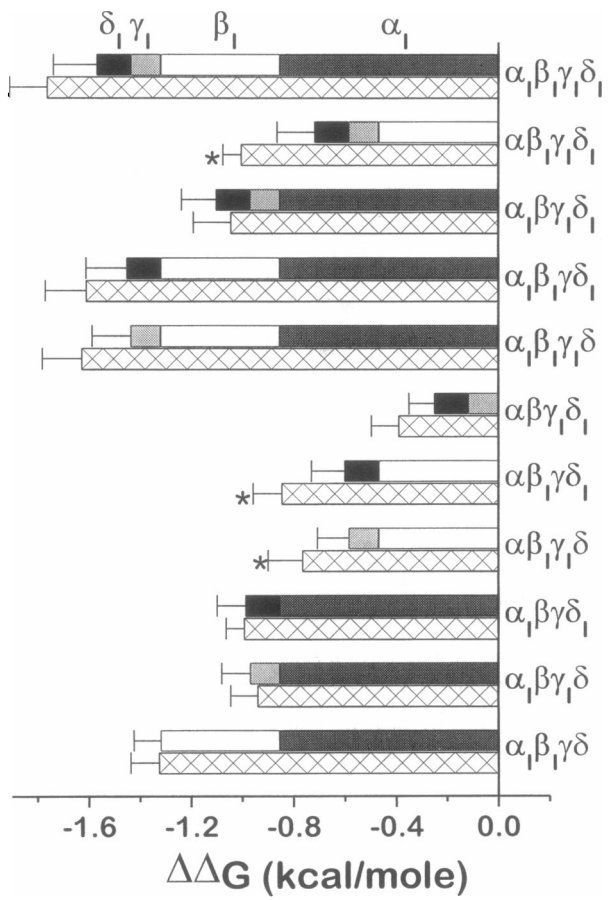

FIGURE 3 Hexanol binding energy effects of coexpressing mutant subunits compared to the sum of individual mutant effects. ▩, Average ± SE of calculated $\Delta\Delta G_{mixture}$ values for receptors containing more than one 10′I mutation, indicated by the subscripted I on the vertical axis labels. Each hatched bar is paired with a stacked bar comprising the $\Delta\Delta G$ values (from Fig. 2) derived for each mutant subunit expressed alone. Each subunit bar is shaded differently and labeled at the top of the figure. The total lengths of the stacked bars represent the sums of component $\Delta\Delta G$'s ($\Sigma\Delta\Delta G_{subunits}$) ± propagated standard errors. *Indicates paired bars differ from each other at $p \leq 0.05$.

value from Fig. 2 (by definition, the $\Delta\Delta G$ contribution of wild-type subunits is 0). For most sets of coexpressed mutant subunits, the two bars are of nearly equal length, demonstrating that the sum of each mutant subunit's $\Delta\Delta G$ contribution to hexanol binding ($\Sigma\Delta\Delta G_{subunits}$) closely predicts the value of $\Delta\Delta G_{mixture}$. In fact, for all but two combinations $\Delta\Delta G_{mixture}$ was greater than $\Sigma\Delta\Delta G_{subunits}$, but this difference is only statistically significant for three mutant mixtures. To assess whether the combined data differ from additivity, Fig. 4 shows $\Sigma\Delta\Delta G_{subunits}$ plotted against $\Delta\Delta G_{mixture}$ and the fitted least-squares line through the data (Wells, 1990). The ideal fit representing energy additivity would be the line of unity. The least-squares fitted line has a slope near 1.0 (0.97 ± 0.09) and an intercept that is not significantly different from zero (0.09 ± 0.11). Thus, despite a consistent trend in the data toward supraadditivity, the results are not significantly different from those predicted by the additivity hypothesis. These results are clearly inconsistent with the presence of multiple exclusive binding sites formed by different subunits. They indicate that hexanol makes simultaneous contact with all nAChR 10′ residues when bound in its channel site.

DISCUSSION

Mutations on all of the nAChR subunits affect hydrophobic blockers

Considered together with previous studies, the present study confirms a model in which hydrophobic alcohols and anesthetics inhibit nAChR channel function by binding within the open channel at a discrete site. For all of the single-subunit mutant receptors where hydrophobicity of the M2 10′ side chain was altered, the qualitative effects on hydrophobic blockers are consistent. When hydrophobicity of the 10′ side chain increases (i.e., isoleucine mutants), apparent channel sensitivity to both hexanol and octanol is enhanced (Fig. 1). When the side-chain hydrophobicity decreases (γ and δ 10′S mutants), apparent channel sensitivity to alcohols is reduced (Fig. 2). Comparison of octanol inhibition kinetics in wild-type and αS10′I mutant receptors suggests that changes in octanol sensitivity are due to altered rates of dissociation (k_{off}) from its binding site. These data are consistent with a model in which each of the 10′ side chains is close enough to interact via the hydrophobic effect with blocker molecules within the channel.

Although all of the mutations produce changes in sensitivity to channel blockers, none of them alter the established open-channel state selectivity for this interaction. This is best appreciated in the octanol-inhibited current traces in Fig. 1 (*top*). Octanol is present throughout the rapid-perfusion experiment. Some degree of inhibition of closed nAChR is indicated by the decrease (relative to control current traces) in peak currents immediately after ACh application. After ACh application and channel opening, all of the current traces where octanol is present (wt and mutants) undergo a rapid relaxation toward deeper inhibition within 5–10 ms. The degree of current inhibition is the same, whether octanol is present throughout the experiment or only during ACh application. Thus, for each of the channels studied, the open-channel state is more sensitive to octanol than is the closed-channel state.

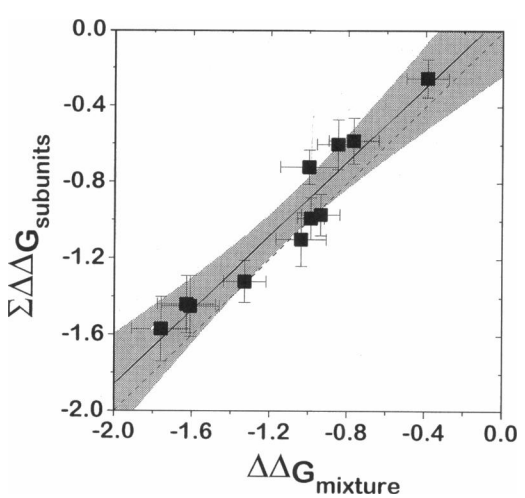

FIGURE 4 Statistical analysis of subunit energy additivity. Paired sets of data from Fig. 3 were plotted on axes representing the $\Delta\Delta G_{hex}$ values derived from receptors coexpressing multiple 10′I mutant subunits (*abscissa*) and the sum of $\Delta\Delta G_{hex}$ values derived from receptors expressing only one 10′I mutant subunit (*ordinate*). Linear least-squares analysis determined the best fit line (——), and 95% confidence limits were calculated and plotted (*shaded area*). The linear least-squares fitted slope is 0.97 ± 0.09, and the intercept is 0.09 ± 0.11. The fitted line does not significantly differ from the line of identity (– – –) over the experimental range of $\Delta\Delta G$ values.

Effects of 10′ mutations on gating

Changes in gating behavior caused by M2 domain mutations at 9′ loci have been described (Filatov and White, 1995; Labarca et al., 1995). Unlike the 9′ loci, where similar mutations cause approximately equal effects on all subunits, the different subunit 10′ isoleucine mutations cause different effects on nAChR channel gating (Table 2). None changes single-channel conductance more than 20%, but effects on mean open-channel lifetimes, apparent ACh affinity, and desensitization are distinctly different.

The changes in K_{ACh} associated with different 10′I mutations cause bias in the comparison of apparent hexanol binding energy effects between different mutant receptors. With the γA10′I mutation, the mean channel lifetime is increased relative to wild type (Table 2). Thus this mutation appears to stabilize the open-channel state relative to the closed state, resulting in a low apparent K_{ACh}. In contrast, single-channel openings of the βT10′I mutant are shorter than those of wild-type nAChR, suggesting a relatively unstable open channel and concomitant increase in apparent K_{ACh}. Because alcohols bind preferentially to the open-channel state, they will stabilize this state relative to the closed-channel state. In βT10′I, with a lower open state

stability than wild type, alcohols will allosterically shift closed states toward the open state, resulting in a lower apparent alcohol inhibition than would be observed if the open channel had the same stability as the wild-type channel. On the other hand, stable open states (e.g., γA10′I) will not have the same degree of alcohol-induced shift, because the equilibrium between closed-liganded channels and open channels is estimated to be nearly 100% toward the open state in native nicotinic receptors (Ogden and Colquhoun, 1983). Thus the hexanol sensitivity of the βT10′I receptor's open state may be underestimated relative to the other mutant receptors that display reduced K_{ACh} and stable open states.

Asymmetry in nAChR subunit interactions with alcohols

Models of the nAChR pore have, for the most part, emphasized the fivefold symmetry seen in photomicrographs of the receptor (Unwin, 1993). Photolabeling and mutagenesis experiments are generally consistent with an α-helical secondary structure in the M2 domains (Revah et al., 1990; Charnet et al., 1990; White and Cohen, 1992; Akabas et al., 1994). Based on these assumptions, the nAChR pore is frequently modeled as a series of "rings" formed by homologous 2′, 6′, 10′, and 14′ M2 side chains, which are thought to be oriented toward the water-filled lumen. Nonetheless, examples of quantifiable pore features that have equal contributions from all five subunits are few. The best example is the 9′ "leucine ring," in which mutation of any of the homologous leucines to threonine or serine contributes approximately equal amounts of energy to the gating process (Filatov and White, 1995; Labarca et al., 1995). Another example where symmetry appears to apply is at 6′ and 10′ rings, where serine-to-alanine mutations on each subunit affect the interaction of the charged blocker QX-222 roughly equally (Charnet et al., 1990). However, not all subunit mutations were studied at each "ring," and the observed effects of individual mutations in these studies were quite small (30–50% change in apparent K_d), so that discerning between additive and nonadditive energetics is difficult (see below). Asymmetrical contributions to ionic conductance and selectivity by the pore have been reported at either end (−2′, −1′, 2′, and 20′ loci) of the M2 domains (Cohen et al., 1992a,b; Villarroel et al., 1992; Kienker et al., 1994).

If all of the subunit M2 10′ side chains are oriented symmetrically facing the hydrophobic blocker site, and if mutation of these residues does not significantly change this orientation, then an equivalent mutation on any single subunit should cause an equal change in blocker binding energy. Instead, this study demonstrates that similar mutations on different 10′ subunit side chains result in quantitatively unequal effects on hexanol binding. The apparent $\Delta\Delta G_{hex}$ effect of the αS10′I mutation is roughly twice that of the βT10′I mutation (Fig. 2), consistent with the idea that the 10′ side chains from two α-subunits and one β-subunit make about equal molecular contact with hexanol in its pore site. In contrast, the apparent $\Delta\Delta G_{hex}$ effects of S→I mutations on both the γ- and δ-subunits are less than half those associated with equivalent mutations on α- or β-subunits. Considered together with the finding that alcohols simultaneously interact with all subunits when blocking current, the data suggest that, compared to α- and β-residues, the γ- and δ-subunit M2 10′ residues make less contact with hydrophobic blockers.

The most critical factor in discerning asymmetrical subunit interactions with either permeant ions or nonpermeant channel blockers is the ability to precisely measure changes in receptor function induced by subunit mutations. The present study enhanced its sensitivity to asymmetry in two ways. First, the degree of hydrophobicity changes in the mutations used here was large, resulting in changes as great as fivefold in the apparent binding of hydrophobic blockers for a single subunit mutation. Nonequivalent mutations among the four subunit types were corrected to the extent possible by studying pairs of mutants that together produced the same overall change in side chain. Second, rapid patch perfusion provides ideal quantitation of receptor occupancy by blockers in the open state, because agonist and blocker concentration jumps can be achieved on a time scale faster than receptor desensitization.

Could the apparently weak interaction of γ- and δ-subunits be an artifact from the assembly of nAChRs lacking these mutated subunits? It is known that nAChRs lacking either γ- or δ-subunits can form functional channels in *Xenopus* oocytes (Charnet et al., 1992; Jackson et al., 1990; Lo et al., 1990). Several observations argue against this possibility. First, currents obtained from whole oocytes expressing γ-less and δ-less nAChRs are generally much smaller than those from receptors containing all subunits. In this study, the expression of the cRNA mixtures containing γ- and δ-subunit mutations was only moderately smaller than wild-type nAChR in whole oocytes, and macroscopic currents were routinely obtained from patches. Furthermore, oocytes coexpressing both γ- and δ-mutant subunits produced patch-detectable currents, whereas there are no reports of nAChRs forming functional channels in the absence of both of these subunits. Finally, the effects of γ- and δ-subunit mutations, although small, were consistent and additive with other subunit effects. Effects due to the absence of these subunits are less likely to be additive, because receptors formed in their absence presumably use other (cRNA-encoded or endogenous; Buller and White, 1990) subunits to replace them.

There is no way to establish whether the 10′ mutations on γ- and δ-subunits induce significant changes in side-chain orientation relative to the receptor pore. For example, the wild-type alanine side chains may face toward the water-filled pore, whereas isoleucines at these sites may become buried within the protein, reducing the unfavorable interaction with water. Arguing against this possibility is the observation that both increasing and decreasing hydrophobic-

ity at these sites produces opposite, albeit small changes in hexanol sensitivity.

Subunit energy contributions are additive

The second important observation derived from coexpression of mutant subunits is that their apparent energy contributions to hexanol inhibition are additive (Figs. 3 and 4). This observation indicates that subunit interactions with alcohols in the pore are both independent and simultaneous (Wells, 1990; Heginbotham and MacKinnon, 1992).

To illustrate this conclusion, consider the implication of the observed energy additivity on the behavior of apparent blocker affinities. Energy additivity for the 5-subunits of nAChR can be summarized as

$$\Delta G_{tot} = \sum_{i=1}^{5} \Delta G_i, \qquad (1a)$$

where $\Delta G = -RT \ln K$ (R is the gas constant, T is absolute temperature, K_{obs} is the apparent blocker dissociation constant of the receptor, and K_i represents the effective dissociation constant for each subunit contributing to binding). Thus,

$$\Delta G_{tot} = -RT \ln K_1 K_2 \ldots K_5 = -RT \ln K_{obs} \qquad (1b)$$

and

$$K_{obs} = K_\alpha^2 K_\beta K_\gamma K_\delta. \qquad (1c)$$

Energy additivity is present when the effect of coexpressing mutations on different subunits is to multiply their individual effects on the overall dissociation constant. This is clearly seen in an example from the data. The αS10′I mutation causes a 4.3-fold decrease in K_{hex} from wild type, whereas the βT10′I mutation causes a 2.2-fold decrease. The coexpressed αS10′I-βT10′I receptor has 10-fold lower K_{hex} than wild type, very close to that predicted by multiplying the individual subunit effects ($4.3 \times 2.2 = 9.46$). Assuming that each of the two α-subunit mutations contribute equally to hexanol binding, Eq. 1 suggests that each α and β 10′I mutation additively contributes about −0.43 kcal/mol of binding energy to hexanol in the pore, corresponding to an average 2.1-fold decrease in K_{hex} per mutation.

In contrast, consider a model in which each subunit forms an independent site and occupation of each site is mutually exclusive. Blocker occupancy at each site will be determined by its affinity; high-affinity sites will be occupied more, and low-affinity sites less of the time. The overall dissociation constant will be an affinity-weighted average:

$$K_{obs} = \left[\sum_{i=1}^{5}\left(\frac{1}{K_i}\right)\right]^{-1} = \left[\frac{2}{K_\alpha} + \frac{1}{K_\beta} + \frac{1}{K_\gamma} + \frac{1}{K_\delta}\right]^{-1}. \qquad (2)$$

In this "competing sites" model, mutations that enhance blocker interactions with one site will detract from interactions with the other sites; the coexpression of two enhancing mutations on different subunits will result in a K_{obs} change lower than that obtained by multiplying the individual subunit effects.

Returning to the example cited above, the αS10′I-βT10′I receptor result is not consistent with the competing sites model. From Eq. 2, the observed 2.2-fold decrease in K_{hex} for the βT10′I receptor would require that the dissociation constant of the independent site on the β-subunit (K_β) undergo a sevenfold decrease (assuming all of the subunit sites were initially equivalent). Similarly, the observed 4.3-fold effect of the αS10′I mutation requires K_α to decrease by about ninefold. When these altered values are used to predict the effect of αS10′I-βT10′I coexpression, Eq. 2 predicts that K_{hex} will decrease by only 5.4-fold from wild type, far less than the experimentally observed change. This analysis gives similar results when K_γ and K_δ are increased to reflect their small contributions to hexanol binding.

Equations 1c and 2 also demonstrate why less dramatic hydrophobic mutations are not likely to discern between energy additivity and competitive site models. Again assuming that all wild-type subunits have equal K_i values, Eq. 2 predicts a 30% decrease in K_{obs} (about the amount seen in QX-222 studies) if a single subunit mutation causes a 2.5-fold decrease in one subunit site's dissociation constant. Combining two such mutations would give a total of a 1.6-fold decrease in K_{obs} in Eq. 2, whereas the additive model (Eq. 1c) predicts an overall 1.7-fold change in K_{obs}. The two results are barely different.

The observation of energy additivity in our data is inconsistent with a model in which multiple inhibition sites compete for alcohol binding in the pore. All of the subunits must be simultaneously interacting with the blocker. The additivity observation cannot formally rule out models in which multiple alcohol sites can simultaneously bind different alcohol molecules, but the consistently low Hill coefficients for hexanol concentration responses (n_H range for all receptors is 1.0–1.5) suggest that a single site is present.

Most of the coexpressed 10′I subunit mutant receptors cause larger apparent $\Delta\Delta G_{hex}$ than predicted by adding individual subunit $\Delta\Delta G$ values. The additional apparent alcohol binding energy is significant only for a subset of mutant subunit combinations, particularly those where βT10′I is coexpressed with γA10′I or δA10′I (Fig. 3). The βT10′I mutation may cause small changes in the relative positions of other M2 domains or changes in the effective size or position of the alcohol-binding site in the pore. Nevertheless, the trend toward supraadditivity does not reach statistical significance for the data set taken as a whole (Fig. 4), and any synergistic interaction energy is relatively small compared to the strictly additive component.

A model for the hydrophobic blocker site in the nAChR pore

The two major findings of this study are consistent with a central pore site for hydrophobic blockers of the nAChR,

but require modification of the usual symmetry assumptions applied to pore models. The observation that mutation-induced changes in alcohol binding energy are additive among the nAChR subunits indicates that all of the subunits are simultaneously in contact with hydrophobic blockers in their site. The simplest model that accounts for this feature is a central site in the pore formed by all subunit M2 domains. The data are also consistent with the generally accepted model incorporating two α-subunit M2 domains around the nAChR pore; each of the two 10′ side chains from α-subunits and the single 10′ side chain from the β-subunit make roughly the same contact with hydrophobic blockers. The markedly smaller effects of equivalent 10′ mutations on the γ- and δ-subunits lead to the conclusion that the 10′ side chains do not all interact equally with hydrophobic blockers. Assuming that hydrophobic blockers occupy the center of the pore, there must be asymmetry among the 10′ side-chain positions forming the blocker site. γ and δ 10′ side chains may be shifted along the transmembrane axis above or below the α and β side chains, or they may not face as directly toward the ion channel lumen. Alternatively, the blocker site could be located asymmetrically in the pore, perhaps in a pocket formed mostly by α- and β-subunits.

I thank Carol Gelb and Mark Jurman for help with mutagenesis and Gary Yellen for his comments on the manuscript. Jim McLaughlin kindly provided pSP64T plasmids containing the wild-type nAChR subunits. The cDNA for βT10′I was generously provided by Cesar Labarca.

SAF was supported by grants from The Medical Foundation/Charles A. King Trust and the National Institute on Alcohol Abuse and Alcoholism (1-K21-AA00206-01).

REFERENCES

Adams, P. R. 1976. Drug blockade of open end-plate channels. *J. Physiol. (Lond.).* 260:531–552.

Akabas, M. H., C. Kaufmann, P. Archdeacon, and A. Karlin. 1994. Identification of acetylcholine receptor channel-lining residues in the entire M2 segment of the alpha subunit. *Neuron.* 13:919–927.

Buller, A. L., and M. M. White. 1990. Functional acetylcholine receptors expressed in Xenopus oocytes after injection of Torpedo beta, gamma, and delta subunit RNAs are a consequence of endogenous oocyte gene expression. *Mol. Pharmacol.* 37:423–428.

Charnet, P., C. Labarca, R. J. Leonard, N. J. Vogelaar, L. Czyzyk, A. Gouin, N. Davidson, and H. A. Lester. 1990. An open-channel blocker interacts with adjacent turns of alpha-helices in the nicotinic acetylcholine receptor. *Neuron.* 4:87–95.

Charnet, P., C. Labarca, and H. A. Lester. 1992. Structure of the gammaless nicotinic acetylcholine receptor: learning from omission. *Mol. Pharmacol.* 41:708–717.

Cohen, B. N., C. Labarca, L. Czyzyk, N. Davidson, and H. A. Lester. 1992a. $Tris^+/Na^+$ permeability ratios of nicotinic acetylcholine receptors are reduced by mutations near the intracellular end of the M2 region. *J. Gen. Physiol.* 99:545–572.

Cohen, B. N., C. Labarca, N. Davidson, and H. A. Lester. 1992b. Mutations in M2 alter the selectivity of the mouse nicotinic acetylcholine receptor for organic and alkali metal cations. *J. Gen. Physiol.* 100: 373–400.

Devillers-Thiery, A., J. L. Galzi, J. L. Eisele, S. Bertrand, D. Bertrand, and J. P. Changeux. 1993. Functional architecture of the nicotinic acetylcholine receptor: a prototype of ligand-gated ion channels. [Review]. *J. Membr. Biol.* 136:97–112.

Dilger, J. P., and R. S. Brett. 1991. Actions of volatile anesthetics and alcohols on cholinergic receptor channels. *Ann. N.Y. Acad. Sci.* 625: 616–627.

Dilger, J. P., R. S. Brett, and L. A. Lesko. 1991. Effects of isoflurane on acetylcholine receptor channels. 1. Single-channel currents. *Mol. Pharmacol.* 41:127–133.

Filatov, G. N., and M. M. White. 1995. The role of conserved leucines in the M2 domain of the acetylcholine receptor in channel gating. *Mol. Pharmacol.* 48:379–384.

Finer-Moore, J., and R. M. Stroud. 1984. Amphipathic analysis and possible formation of the ion channel in an acetylcholine receptor. *Proc. Natl. Acad. Sci. USA.* 81:155–159.

Forman, S. A., K. W. Miller, and G. Yellen. 1995. A discrete site for general anesthetics on a postsynaptic receptor. *Mol. Pharmacol.* 48: 574–581.

Giraudat, J., M. Dennis, T. Heidmann, J. Y. Chang, and J. P. Changeux. 1986. Structure of the high-affinity binding site for noncompetitive blockers of the acetylcholine receptor: serine-262 of the delta subunit is labeled by [^{3}H]chlorpromazine. *Proc. Natl. Acad. Sci. USA.* 83: 2719–2723.

Giraudat, J., M. Dennis, T. Heidmann, P. Y. Haumont, F. Lederer, and J. P. Changeux. 1987. Structure of the high-affinity binding site for noncompetitive blockers of the acetylcholine receptor: [^{3}H]chlorpromazine labels homologous residues in the beta and delta chains. *Biochemistry.* 26:2410–2418.

Heginbotham, L., and R. MacKinnon. 1992. The aromatic binding site for tetraethylammonium ion on potassium channels. *Neuron.* 8:483–491.

Hucho, F., W. Oberthur, and F. Lottspeich. 1986. The ion channel of the nicotinic acetylcholine receptor is formed by the homologous helices M II of the receptor subunits. *FEBS Lett.* 205:137–142.

Imoto, K., C. Busch, B. Sakmann, M. Mishina, T. Konno, J. Nakai, H. Bujo, Y. Mori, K. Fukuda, and S. Numa. 1988. Rings of negatively charged amino acids determine the acetylcholine receptor channel conductance. *Nature.* 335:645–648.

Imoto, K., T. Konno, J. Nakai, F. Wang, M. Mishina, and S. Numa. 1991. A ring of uncharged polar amino acids as a component of channel constriction in the nicotinic acetylcholine receptor. *FEBS Lett.* 289: 193–200.

Jackson, M. B., K. Imoto, M. Mishina, T. Konno, S. Numa, and B. Sakmann. 1990. Spontaneous and agonist-induced openings of an acetylcholine receptor channel composed of bovine α-, β-, and δ-subunits. *Pflugers Arch.* 417:129–135.

Karlin, A., P. N. Kao, and M. DiPaola. 1986. Molecular pharmacology of the nicotinic acetylcholine receptor. *Trends Pharmacol. Sci.* 7:304–308.

Kienker, P., G. Tomaselli, M. Jurman, and G. Yellen. 1994. Conductance mutations of the nicotinic acetylcholine receptor do not act by a simple electrostatic mechanism. *Biophys. J.* 66:325–334.

Kistler, J., R. M. Stroud, W. Klymkowsky, R. A. Lalancette, and R. H. Fairclough. 1982. Structure and function of an acetylcholine receptor. *Biophys. J.* 37:371–383.

Krieg, P. A., and D. A. Melton. 1984. Functional messenger RNAs are produced by SP6 in vitro transcription of cloned cDNAs. *Nucleic Acids. Res.* 12:7057–7070.

Labarca, C., M. W. Nowak, H. Zhang, L. Tang, P. Deshpande, and H. A. Lester. 1995. Channel gating governed symmetrically by conserved leucine residues in the M2 domain of nicotinic receptors. *Nature.* 376: 514–516.

Lechleiter, J., and R. Gruener. 1984. Halothane shortens acetylcholine receptor channel kinetics without affecting conductance. *Proc. Natl. Acad. Sci. USA.* 81:2929–2933.

Leonard, R. J., C. G. Labarca, P. Charnet, N. Davidson, and H. A. Lester. 1988. Evidence that the M2 membrane-spanning region lines the ion channel pore of the nicotinic receptor. *Science.* 242:1578–1581.

Liu, Y., and J. P. Dilger. 1991. Opening rate of acetylcholine receptor channels. *Biophys. J.* 60:424–432.

Lo, D. C., J. L. Pinkham, and C. F. Stevens. 1990. Influence of the gamma subunit and expression system on acetylcholine receptor gating. *Neuron.* 5:857–866.

McLarnon, J. G., P. Pennefather, and D. M. J. Quastel. 1988. Mechanisms of nicotinic channel blockade by anesthetics. *In* Molecular and Cellular Mechanisms of Anesthetics. S. H. Roth and K. W. Miller, editors. Plenum Publishing Corp., New York. 155–164.

Miller, C. 1989. Genetic manipulation of ion channels: a new approach to structure and function. *Neuron.* 2:1195–1205.

Nelson, R. M., and G. L. Long. 1989. A general method of site-specific mutagenesis using a modification of the *Thermus aquaticus* polymerase chain reaction. *Anal. Biochem.* 180:147–151.

Ogden, D. C., and D. Colquhoun. 1983. The efficacy of agonists at the frog neuromuscular junction studied with single channel recording. *Pflugers Arch.* 399:246–248.

Pedersen, S. E., S. D. Sharp, W. S. Liu, and J. B. Cohen. 1992. Structure of the noncompetitive antagonist-binding site of the Torpedo nicotinic acetylcholine receptor. [^{3}H]meproadifen mustard reacts selectively with alpha-subunit Glu-262. *J. Biol. Chem.* 267:10489–10499.

Revah, F., J. L. Galzi, J. Giraudat, P. Y. Haumont, F. Lederer, and J. P. Changeux. 1990. The noncompetitive blocker [^{3}H]chlorpromazine labels three amino acids of the acetylcholine receptor gamma subunit: implications for the alpha-helical organization of regions MII and for the structure of the ion channel. *Proc. Natl. Acad. Sci. USA.* 87:4675–4679.

Sankararamakrishnan, R., C. Adcock, and M. S. P. Sansom. 1996. The pore domain of the nicotinic acetylcholine receptor: molecular modeling, pore dimensions, and electrostatics. *Biophys. J.* 71:1659–1671.

Tomaselli, G. F., J. T. McLaughlin, M. E. Jurman, E. Hawrot, and G. Yellen. 1991. Mutations affecting agonist sensitivity of the nicotinic acetylcholine receptor. *Biophys. J.* 60:721–727.

Unwin, N. 1993. Nicotinic acetylcholine receptor at 9 Å resolution. *J. Mol. Biol.* 229:1101–1124.

Villarroel, A., S. Herlitze, M. Koenen, and B. Sakmann. 1991. Location of a threonine residue in the alpha-subunit M2 transmembrane segment that determines the ion flow through the acetylcholine receptor channel. *Proc. R. Soc. Lond. B.* 243:69–74.

Villarroel, A., S. Herlitze, V. Witzemann, M. Koenen, and B. Sakmann. 1992. Asymmetry of the rat acetylcholine receptor subunits in the narrow region of the pore. *Proc. R. Soc. Lond. B.* 249:317–324.

Wells, J. A. 1990. Additivity of mutational effects in proteins. *Biochemistry.* 29:8509–8517.

White, B. H., and J. B. Cohen. 1992. Agonist-induced changes in the structure of the acetylcholine receptor M2 regions revealed by photoincorporation of an uncharged nicotinic noncompetitive antagonist. *J. Biol. Chem.* 267:15770–15783.

Wood, S. C., P. H. Tonner, A. J. de Armendi, B. Bugge, and K. W. Miller. 1995. Channel inhibition by alkanols occurs at a binding site on the nicotinic acetylcholine receptor. *Mol. Pharmacol.* 47:121–130.